

# TiO<sub>2</sub> thin films on soda-lime and borosilicate glass prepared by sol-gel processing: influence of the substrates

Andreas Bittner · Rainer Jahn · Peer Löbmann

Received: 10 September 2010/Accepted: 10 January 2011/Published online: 19 January 2011  
© Springer Science+Business Media, LLC 2011

**Abstract** TiO<sub>2</sub> films were deposited on soda-lime and borosilicate glass substrates, their optical and microstructural properties were investigated. X-ray diffraction showed significant differences between the sample series. Films deposited on the upper surface of soda-lime glass substrates showed higher indices of refraction than those prepared on the lower surface that had been in contact with the tin bath during float glass production. Results indicate that these differences not only result from different optical properties of the TiO<sub>2</sub> backbone material due to alkali contamination but that also different film porosities can be measured by ellipsometric porosimetry.

**Keywords** Titanium dioxide · Thin films · Glass substrates · Optical properties · Ellipsometric porosimetry

## 1 Introduction

The composition of glass substrates can have a crucial impact on the deposition and properties of coatings. Even though film growth rates during atomic layer deposition experiments are higher on soda-lime than on borosilicate glass [1], the effect of high alkali contents is mostly adverse: sodium diffusion is known to impede the electric conductivity [2] or photocatalytical activity [3, 4] of

functional films. As early as in 1967 it was recognized that the refractive index of sol-gel deposited TiO<sub>2</sub> is diminished by Na ions [5], for films <75 nm the formation of crystalline material may completely be suppressed [6].

As glass sheets nowadays are almost exclusively produced by floating on a melt of tin, in addition to their compositional characteristics the properties of their surfaces may be different whether they were exposed to the atmosphere or to the liquid metal during processing. X-ray reflectivity experiments reveal that these changes are less pronounced for borosilicate substrates than for soda-lime glass [7, 8]. As tin diffuses several micrometers into the glass [9], the refractive index of the lower surface increases [7, 8, 10, 11] and the coefficient of thermal expansion decreases [10, 11]. In addition, it can be observed that the interdiffusion of K<sup>+</sup> and Na<sup>+</sup> during the chemical hardening of glasses is slowed down in the presence of tin [11]. Consequently sodium ions are more easily leached from the upper surface of soda-lime glass [12], therefore this side also turns out to be more susceptible to weathering in outdoor exposure testing [13].

General aspects of thermal densification and microstructural evolution of TiO<sub>2</sub> thin films prepared by sol-gel processing have already been discussed [14]. In this paper the specific influence of soda-lime and borosilicate surfaces is systematically investigated.

## 2 Experimental procedure

As previously reported [15], coating solutions were prepared from soluble precursor powders [16] with an oxide yield respective to crystalline TiO<sub>2</sub> of 6 mass%. The solvent mixture used in this study contained 90 mass% ethanol and 10 mass% 1,5-pentanediol.

A. Bittner  
Lehrstuhl für chemische Technologie der Materialsynthese,  
Universität Würzburg, Röntgenring 11, 97070 Würzburg,  
Germany

R. Jahn · P. Löbmann (✉)  
Fraunhofer-Institut für Silicatforschung, Neunerplatz 2, 97082  
Würzburg, Germany  
e-mail: peer.loebmann@isc.fraunhofer.de

Thin films were prepared by dip coating on soda-lime glass (Optiwhite, Pilkington NSG) and borosilicate glass (Schott, Borofloat®) at the size of  $3.3 \times 150 \times 100$  mm<sup>3</sup>. Substrates were pre-cleaned in a laboratory dishwasher by an alkaline cleaning procedure and a final neutralization step immediately before the coating experiments. After 5 min holding time in the coating chamber the afore coated samples (withdraw rate 20 cm/min) were pre-dried for 10 min at 80°C in a vented furnace (Model D-6450, Heraeus Instruments, Hanau, Germany). Calcination ensued by rapid thermal annealing for 10 min at 300–600°C in a pre-heated vented air oven (Model Thermicon P, Heraeus Instruments, Hanau, Germany) and slow cooling down in the furnace after switching off the power supply.

Grazing incidence X-ray diffractometry (GIXRD) was performed with a Siemens D-5005 diffractometer (Bruker AXS GmbH, Karlsruhe, Germany) at the angle of incidence of 0.5° and at an angular range of 23°–27.5°.

Scanning electron microscopy (SEM) was performed using a Zeiss Supra 25 (Carl Zeiss SMT, Oberkochen, Germany).

Refractive index  $n_{(550 \text{ nm})}$  and film thickness ( $t$ ) were determined by UV–Vis spectroscopy as well as ellipsometry. In both methods, different dispersions for the respective surface of the soda-lime glass substrate were considered. With the UV–Vis spectrometer (Shimadzu UV-3100, Kyoto, Japan) the spectral range of 300–2,400 nm was measured. The two evaluable maxima of reflection that had been detected were used to calculate the respective reflective indices, using Fresnel equations for vertical incidence and the interference law. To achieve the refractive index for a wavelength of 550 nm, both results were fitted with an advanced Cauchy dispersion curve. Ellipsometric measurements were performed by a GES-SE instrument (Sopra, Paris, France). Results were calculated using the software “WinElli\_II”. The measured functions alpha and beta were fitted in the range of 1.3–3.1 eV on the supposition of a double layer model, using Cauchy’s equation for dispersion. By way of illustration the ascertained values are shown as a weighted average.

Open porosity was determined with atmospheric ellipsometric porosimetry (EP-A), which uses the change of optical characteristics during the water vapor adsorption and desorption, to calculate the open porosity. Therefore, the ellipsometric results obtained for completely empty pores ( $n_1$ ) and fully water-filled pores ( $n_2$ ) were evaluated with Lorentz–Lorenz equation, without requirement of any information of the bulk material.

$$P_L = \frac{\frac{n_2^2 - 1}{n_2^2 + 2} - \frac{n_1^2 - 1}{n_1^2 + 2}}{\frac{n_{\text{water}}^2 - 1}{n_{\text{water}}^2 + 2}} \quad (\text{Lorentz – Lorenz})$$

Also overall porosity could be evaluated from the refractive index provided by UV–Vis spectrometry using Lorentz–Lorenz equation [17] or the expressions proposed by Matsubara [18] and Yoldas [19]. These calculations are based on the estimation of dense anatase crystallites ( $n = 2.54$  for  $\lambda = 550$  nm) as backbone material.

$$P_L = 1 - \frac{n_{UV-Vis}^2 - 1}{n_{UV-Vis}^2 + 2} \frac{n_{anatase}^2 + 2}{n_{anatase}^2 - 1} \quad (\text{Lorentz – Lorenz})$$

$$P_M = \frac{n_{UV-Vis} - n_{anatase}}{1 - n_{anatase}} \quad (\text{Matsubara})$$

$$P_Y = 1 - \frac{n_{UV-Vis}^2 - 1}{n_{anatase}^2 - 1} \quad (\text{Yoldas})$$

XPS measurements were performed on a X-Ray photoelectron spectrometer (model X-Probe, Surface Science Instruments, California) using monochromated Al K $\alpha$  radiation. For depth profiling a sputtering source (Leybold-Heraeus Model IQE) at operation voltage 5 kV was used.

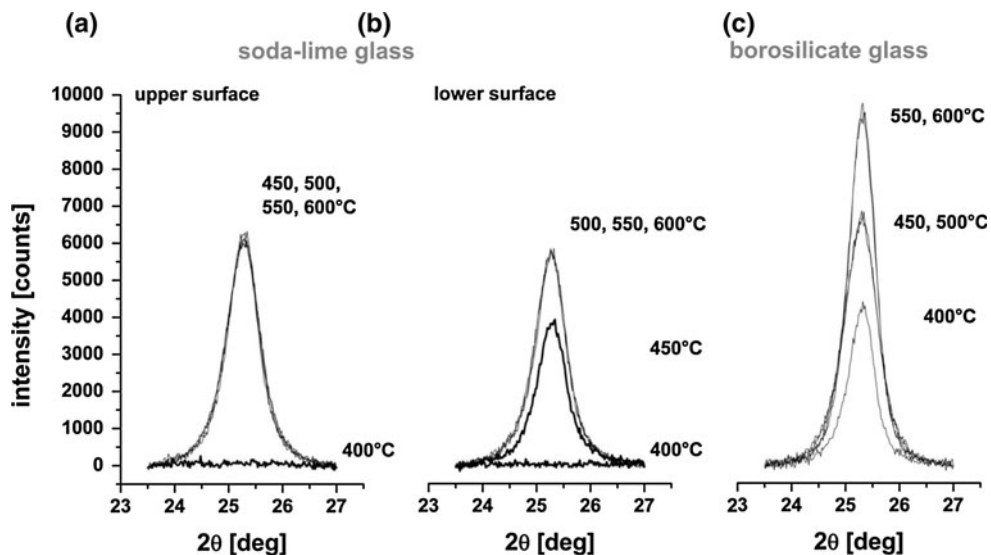
### 3 Results and discussion

The X-ray diffraction pattern of TiO<sub>2</sub> films as a function of annealing temperature was measured. Samples treated at 400°C are amorphous, at higher temperatures signals corresponding to the anatase phase become apparent. Even after treatment at 600°C no traces of rutile can be detected (data not shown). With final thicknesses of 120 nm the films are by far larger than the ones Yuksel et al. [6] had observed a complete inhibition of crystallization due to the diffusion of alkali ions.

In order to investigate the phase evolution of the films more closely, the (101) reflex at  $2\Theta = 25.66^\circ$  was surveyed (Fig. 1). TiO<sub>2</sub> films deposited on the upper surface of soda-lime substrates (Fig. 1a) show a transition from the amorphous state (400°C) to anatase at 450°C. Above this treatment temperature the reflex intensity does not change significantly any more. In contrast to this, an intermediate intensity is observed after annealing at 450°C on the lower surface (Fig. 1b) before the signals coalesce. This observation indicates a retarded crystallization process. Even though without an internal standard quantitative XRD analysis cannot be performed, the final signal intensity obtained for measurements under identical conditions seems to be slightly lower.

No differences between films deposited on both surfaces could be detected in the case of borosilicate glass (Fig. 1c). In contrast to the films prepared on soda-lime glass, the

**Fig. 1** XRD pattern of  $\text{TiO}_2$  thin films prepared on the upper (a) and the lower (b) surface of soda-lime glass as a function of annealing temperature. No differences between the substrate surfaces were found for  $\text{TiO}_2$  films deposited on borosilicate glass (c)



presence of anatase can already be detected after annealing at 400°C. For treatment temperatures of 450 and 500°C the intensity of the overlapping signals is higher than those of the respective signals of films prepared on soda-lime glass. After sintering at 550 and 600°C another significant increase of intensity is observed.

It was not possible to detect any microstructural differences between films prepared on soda-lime and borosilicate glass by SEM for samples that had undergone identical thermal treatments. In Fig. 2 cross-sectional views of films prepared on the upper and lower surface of soda-lime glass are shown after annealing at 550°C.

The films exhibit a randomly oriented polycrystalline microstructure. Since it is difficult to correctly estimate film porosities and resulting optical properties from electron microscopy, the further investigations were focused on optical spectroscopy.

Corresponding differences regarding their refractive index between the sample series are detected by

ellipsometric spectroscopy (Fig. 3). Irrespective of the substrate type as-deposited films exhibit  $n$ -values of approximately 1.75. Up to 400°C, where the onset of anatase crystallization was detected by XRD, the indices of refraction increase to 2.1–2.2 due to the removal of residual organics from the films [14].

On the lower surface of soda-lime substrates this value is not substantially increased upon annealing at higher temperatures. On the upper surface the refractive index increases from 2.2 to 2.35. It has to be noted, though, that the scattering between data points as determined by ellipsometry is far from being satisfactory. Nevertheless, the difference in optical properties between the films prepared on both sides of soda-lime glass coincides with a higher crystallinity of the  $\text{TiO}_2$  deposited on the upper side as suggested by XRD analysis (Fig. 1 a, b).

For  $\text{TiO}_2$  films prepared on borosilicate substrates there is no significant difference between the upper surface and the lower glass surface that had been in contact with the tin

**Fig. 2** SEM cross-sectional view of  $\text{TiO}_2$  thin films prepared on the upper (a) and lower (b) surface of soda-lime glass after annealing at 550°C

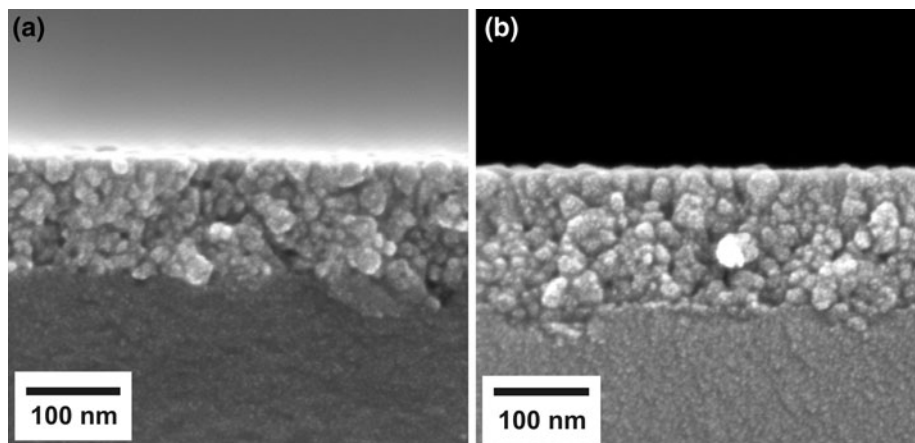
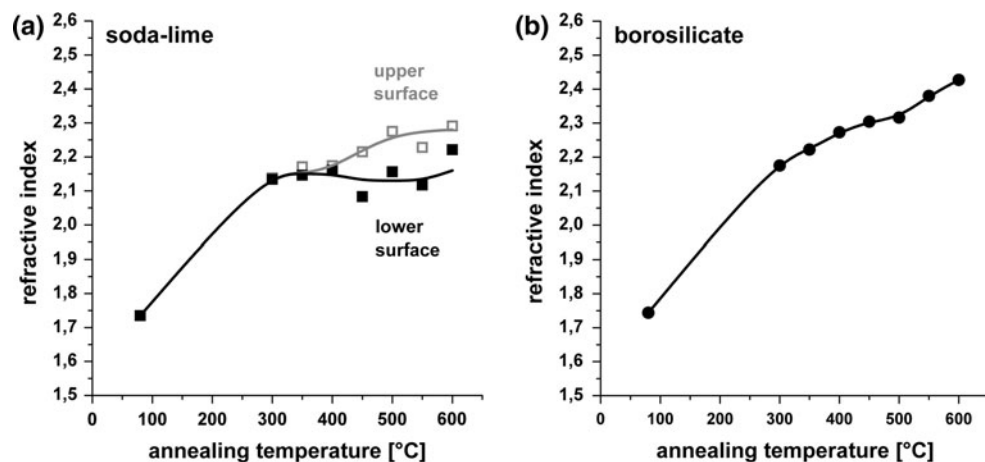


**Fig. 3** Refractive index of  $\text{TiO}_2$  thin films prepared on soda-lime glass (**a**) and borosilicate glass (**b**) as a function of annealing temperature. Samples were measured by spectroscopic ellipsometry on the upper and lower surface of the substrates for films prepared on soda-lime glass. Lines are drawn as guide to the eyes



bath during glass processing. From 400 to 600°C the index of refraction systematically increases to the theoretical value for pure anatase ( $n_{550}=2.54$ ). Since no rutile ( $n_{550}=2.75$ ) has been detected by XRD, the films can be considered to be composed of pure anatase sintered to high density. Borosilicate glass has a lower sodium content (~4.2 mass%  $\text{Na}_2\text{O}$ ) than soda-lime glass (~14 mass%  $\text{Na}_2\text{O}$ ). Therefore it is reasonable to assume a reduced contamination of  $\text{TiO}_2$  and thus a higher refractive index, which is also consistent with the higher crystallinity (Fig. 1). Since borofloat is only affected by molten tin to a small extent [7, 8], no difference between both sides is to be expected.

Due to the disappointing high scattering of data points for soda-lime glass (Fig. 3), refractive indices were supplementarily determined by UV–Vis spectroscopy (Fig. 4) confirming the general trend of spectroscopic ellipsometry. According to the experimental setup, both films of the double-sided substrates are measured which makes it impossible to distinguish individual characteristics. For borosilicate substrates the data derived from UV–Vis measurements correspond well with the results from spectroscopic ellipsometry. In the case of soda-lime glass, the “integral” UV–Vis measurements lie closer to the higher refractive indices measured by ellipsometry on the upper surfaces.

In order to differentiate between the two substrate surfaces of soda-lime glass by UV–Vis spectroscopy, single side coatings were prepared by laminating the opposite side during dip-coating experiments. The respective data are summarized in Fig. 5. The refractive indices measured for the upper and lower surface enclose the “integral” measurement of the double-side coated sample (Fig. 4). Similar to the results derived from spectroscopic ellipsometry (Fig. 3) higher indices of refraction are obtained for the films deposited on the upper side of the soda-lime substrates, but a much steadier course of neighboring data points is obtained.

On first sight the tendency of  $\text{TiO}_2$  to have a higher index of refraction on the top surface seems surprising. Due to the limited diffusivity of sodium in the lower surface region the titania should be better protected from contamination there. One has to keep in mind though, that the upper surface region may well be depleted of alkali ions during aging and the alkaline cleaning procedure.

This interpretation is supported by X-ray photoelectron spectroscopy (XPS) and depth profiling of the films prepared on the different surfaces of soda-lime glass (Fig. 6). For large sputtering times, when the substrate is already penetrated, a higher sodium content is detected for the lower surface of the soda lime glass substrate. Accordingly a higher level of sodium contamination of the  $\text{TiO}_2$  film deposited on the lower surface is measured for shorter sputtering times. As one would expect, traces of Sn are only found on the lower surface that had been in contact with the molten tin bath during glass processing.

Even though changes in the optical properties of  $\text{TiO}_2$  through sodium contamination [5] seem to be the most important reason for the deteriorated index of refraction the fact that also microstructural differences in film morphology may contribute to the phenomenon has to be taken into consideration. Therefore ellipsometric porosimetry (EP) was employed to characterize  $\text{TiO}_2$  films prepared on the upper and lower surface of soda-lime glass. In Fig. 7 water vapor sorption isotherms and the resulting pore radius distributions are given for samples that had been annealed at 550°C.

The  $\text{TiO}_2$  film prepared at the lower surface of the soda-lime glass shows a higher porosity (~9%) than the material deposited on the upper surface (~3%). The pore radius distributions calculated from the isotherms both have a maximum at approximately 2 nm. It has to be acknowledged that EP is able to measure microstructural differences in the films that are not detected by SEM (Fig. 2).

In Fig. 8 the open porosities of  $\text{TiO}_2$  films prepared on the upper and lower surfaces of soda-lime substrates for

**Fig. 4** Refractive index of  $\text{TiO}_2$  thin films prepared on soda-lime glass (**a**) and borosilicate glass (**b**) as a function of annealing temperature as determined by UV–VIS spectroscopy (black lines). For comparison the data points measured by spectroscopic ellipsometry from Fig. 3 are given in grey

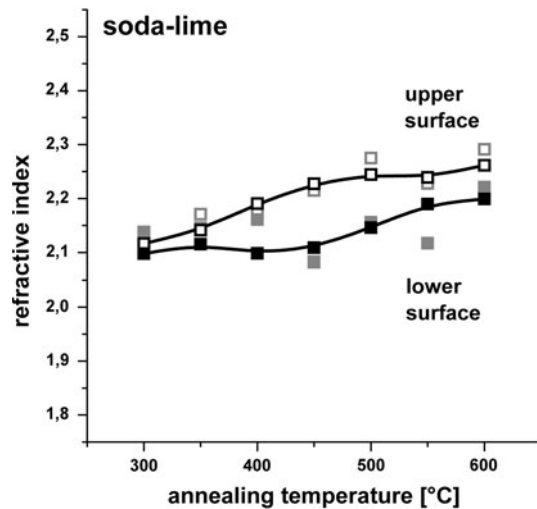
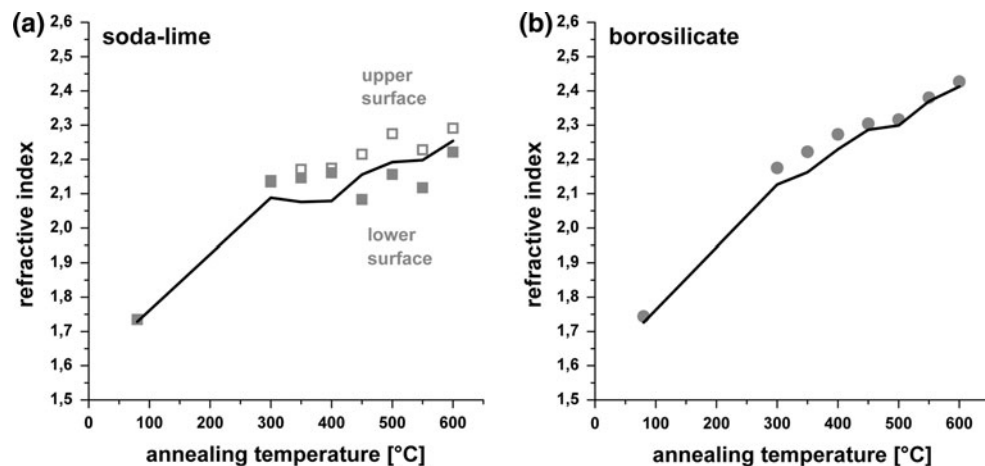


**Fig. 5** Refractive index of  $\text{TiO}_2$  thin films prepared on soda-lime glass as a function of annealing temperature determined by UV–VIS spectroscopy (black lines). Single films were deposited either on the upper or the lower surface of the substrates. For comparison the respective data points measured by spectroscopic ellipsometry from Fig. 3a are given in grey

annealing temperatures between 400 and 600°C are summarized as determined by EP. Additionally the porosities calculated from the respective refractive index (UV–Vis spectroscopy, Fig. 5) are given. It has to be noted that irrespective the method of data analysis the theoretical refractive index of fully crystalline anatase ( $n_{\text{anatase}} = 2.54$ ) is taken as a basis for the backbone film material. As the solid is at least partially amorphous ( $n_{\text{solid}} < n_{\text{anatase}}$ ) at especially lower sintering temperatures, this assumption is inaccurate and the analysis will therefore generally tend to an overestimation of the film porosity.

The porosities determined by UV–Vis spectroscopy in fact are generally higher than the values obtained from EP. Using this method a significant pore volume arises after sintering at 450°C, remains constant up to treatment at 550°C and is diminished again at 600°C. Similar behavior

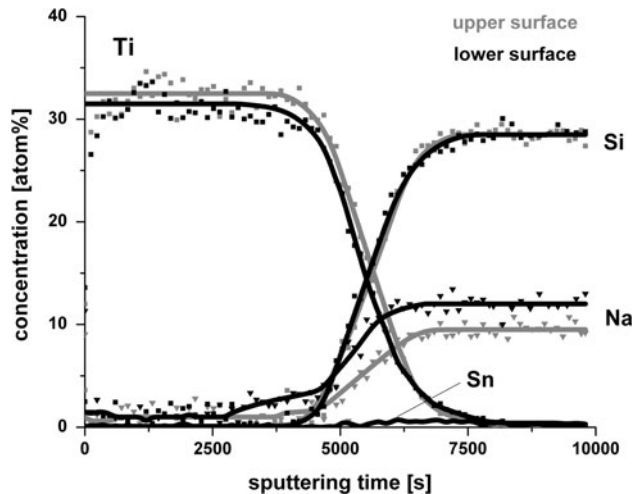


**Fig. 6** XPS depth profile of  $\text{TiO}_2$  thin films prepared on the upper (grey) and lower (black) surface of soda lime glass. The samples were annealed at 550°C, lines are drawn as guide to the eyes

has previously been reported for sol–gel derived powders [20, 21].

The corresponding data of  $\text{TiO}_2$  films on borosilicate glass (Fig. 9) follow the same general trend, but EP does not reveal any structural differences for material deposited on the upper and lower surface of the substrate.

Based on EP a higher pore volume was measured for  $\text{TiO}_2$  thin films deposited on the lower surface of soda-lime substrates (Fig. 8). It must be pointed out that this determination as a start is not based on a postulation regarding the optical properties of the solid phase of the film: At the relative humidity (RH) of 0% the film is considered to be composed of a solid backbone of unknown index and air ( $n_{\text{air}} = 1.0$ ). As RH is increased in the course of the measurement, the pores are successively filled with (a yet unknown amount of) water ( $n_{\text{water}} = 1.33$ ) due to capillary condensation. When RH becomes 100%, a complete filling

**Fig. 7** Sorption isotherms of  $\text{TiO}_2$  films prepared at the upper (open symbols) and lower surface (closed symbols) of soda-lime glass after annealing at 550°C (a) and pore radius distributions derived from the respective desorption branch (b).  $\text{H}_2\text{O}$  vapor sorption was measured by ellipsometric porosimetry, lines are drawn as guide to the eyes

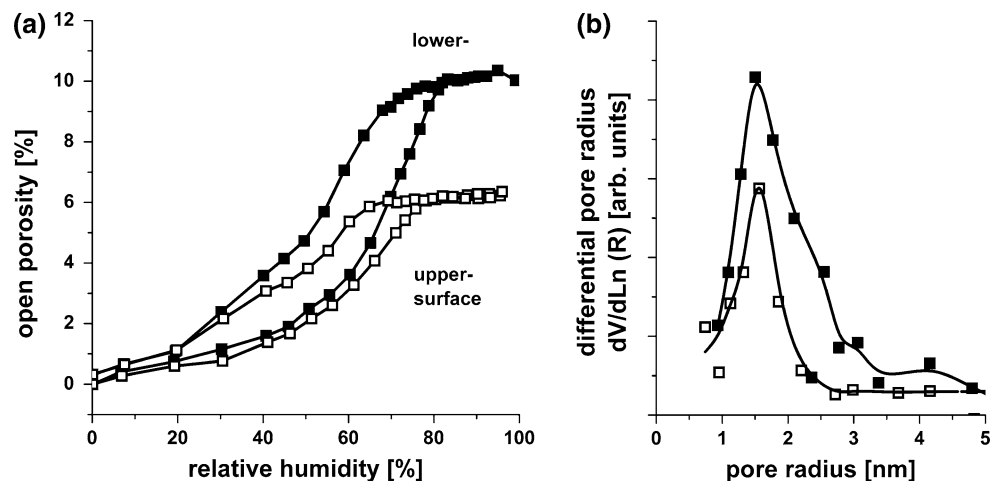


**Fig. 8** Open porosity of  $\text{TiO}_2$  films prepared at the upper (left) and lower (right) surface of soda-lime glass after annealing at different temperatures as determined by ellipsometric porosimetry (line and data markers). Additionally, the porosities from the respective refractive indices (UV–Vis, Fig. 5) calculated according to Yoldas [19], Matsubara [18] and Lorentz–Lorenz [7] are given

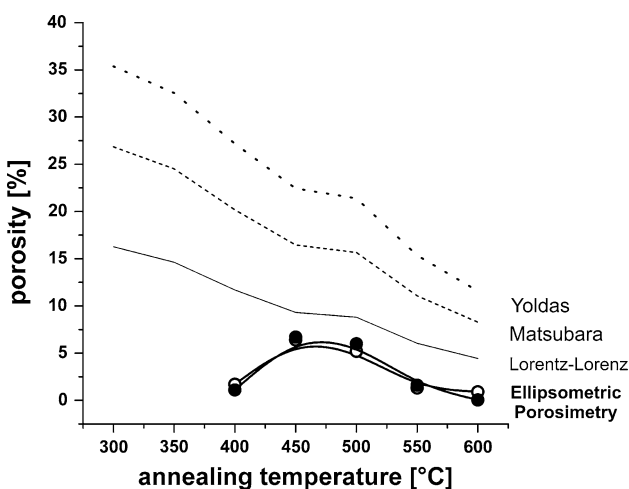
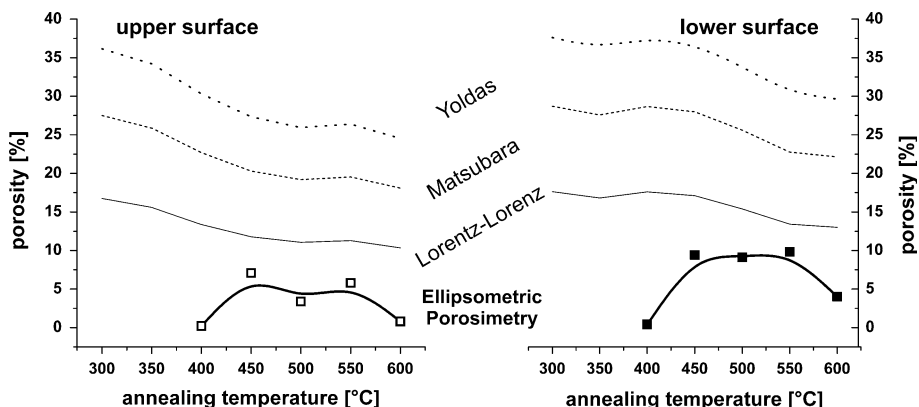


**Fig. 9** Open porosity of  $\text{TiO}_2$  films prepared at the upper (open symbol) and lower (closed symbol) surface of borosilicate glass after annealing at different temperatures as determined by ellipsometric porosimetry. Additionally, the porosities from the respective refractive indices (UV–Vis, Fig. 3) calculated according to Yoldas [19], Matsubara [18] and Lorentz–Lorenz [17] are given

with water is assumed. The absolute film porosity can be calculated as the film properties filled with two known optical media (RH 0%,  $n_{\text{air}} = 1.0$  and RH 100%,  $n_{\text{water}} = 1.33$ ) have been measured. Nevertheless, the term “open porosity” is more appropriate since complete pore accessibility is assumed, therefore, EP is generally prone to underestimate the total porosity [21].

In Fig. 10 the approaches for porosity determination based on UV–Vis spectroscopy and ellipsometric porosity are visualized. Since one method is more likely to overestimate (UV–Vis) and the other to underestimate (EP) the porosity, the “true” values can be expected to be located in the region between the EP measurements and the data provided by UV–Vis spectroscopy.

Based on this careful evaluation it can be concluded that  $\text{TiO}_2$  films prepared on the lower surface of soda-lime glass exhibit a higher porosity than the material deposited on the upper side. This structural difference contributes to the lower refractive index of these films in addition to the lower index of refraction of their “backbone” induced by alkali contamination. In Fig. 11 the index of refraction of solid  $\text{TiO}_2$  “backbone” is given as determined by respective measurements at RH = 0% and RH = 100%. It becomes evident that the  $\text{TiO}_2$  material on the lower surface has a smaller index of refraction than the solid deposited on the other side, presumably due to contamination with alkali

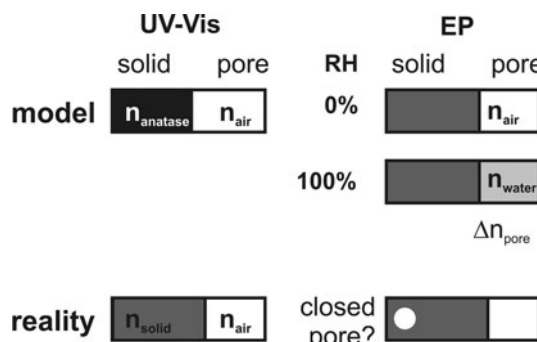


**Fig. 10** Schematic representation of porosity evaluation based on UV-Vis spectroscopy and ellipsometric porosimetry (EP)

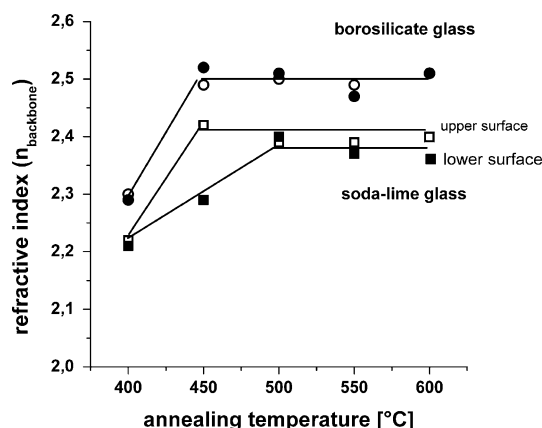


**Fig. 11** Index of refraction of  $\text{TiO}_2$  (“backbone” material) deposited on borosilicate (round symbols) and soda-lime glass substrates (squares). Films were prepared on the upper (open symbols) and lower (closed symbol) surface. Lines are drawn as guide to the eyes

ions. As a consequence of the lower  $\text{Na}_2\text{O}$  content of the substrate,  $\text{TiO}_2$  prepared on borosilicate glass generally exhibits higher refractivities.

#### 4 Conclusions

$\text{TiO}_2$  thin films prepared on borosilicate glass by sol-gel processing show a higher index of refraction compared to material deposited on soda-lime glass due to reduced alkali contamination. No differences were observed on borosilicate for films deposited on the upper or on the lower side that had been in contact with metallic tin during glass production. By contrast, using soda-lime substrates lower indices of refraction are obtained on the lower surface as a consequence of both the contamination of the  $\text{TiO}_2$  and an increased porosity.

**Acknowledgments** The help of Angelika Schmitt in the interpretation of ellipsometer data is gratefully acknowledged.

#### References

- Pore V, Kivel T, Ritala M, Leskel M (2008) Atomic layer deposition of photocatalytic  $\text{TiO}_2$  thin films from  $\text{TiF}_4$  and  $\text{H}_2\text{O}$ . *Dalton Trans* 45:6467–6474
- Davies B, Pannell K, Albright S (1994) Diffusion barrier of sol-gel derived silica for sprayed tin oxide film on soda-lime glass. *J Mater Res* 9(1):226–228
- Paz Y, Heller A (1997) Photo-oxidatively self-cleaning transparent titanium dioxide films on soda-lime glass: the deleterious effect of sodium contamination and its prevention. *J Mater Res* 12(10):2759–2766
- Kim D, Iyoda T, Hashimoto K, Fujishima A (1998) Activity and hardness of supported  $\text{TiO}_2$  films on pyrex and soda-lime glass in photocatalytic degradation of formic acid for 50 days. *J Adv Oxid Technol* 3(2):134–137
- Bach H, Schroeder H (1967) Kristallstruktur und optische Eigenschaften von dünnen organogenen Titanoxyd-Schichten auf Glasunterlagen. *Thin Solid Films* 1:255–276
- Yuksel B, Sam E, Aktas O, Urgen M, Cakir A (2009) Determination of sodium migration in sol-gel deposited titania films on soda-lime glass with r.f. glow discharge optical emission spectroscopy. *Appl Surf Sci* 255:4001–4004
- Anderson O, Daalderop H, Bange K (1997) X-ray reflectivity investigations of glass surfaces produced by float and draw techniques. *Microchim Acta* 125:63–67
- Anderson O, Bange K (1997) Characterization of glass surfaces by X-ray reflectivity. *Glass Sci Technol* 70:316–321
- Williams K, Johnson C, Greengrass J, Tilley B, Gelder D, Johnson J (1997) Tin oxidation state, depth profile of  $\text{Sn}^{2+}$  and  $\text{Sn}^{4+}$  and oxygen diffusivity in float glass by Mössbauer spectroscopy. *J Non-Cryst Solids* 211:164–172
- LeBourhis E (1998) Tin influence on the thermo-mechanical behavior of silico-soda-lime glass. *Verre* 4(4):5–8
- Saggioro B, Ziemath E (2006) Changes of physical properties of glass surfaces exposed to  $\text{KNO}_3$  vapors. *J Non-Cryst Solids* 352:2783–2790
- Solinov V, Temnyakova N, Zinina E, Yuneva E (2008) Water resistance of molded float-glass surfaces. *Glass Ceram* 65:421–423
- Lombardo T, Chabas A, Levèvre R, Verità M, Geotti-Bianchini F (2005) Weathering of float glass exposed outdoors in an urban area. *Glass Technol* 46:271–276
- Bockmeyer M, Löbmann P (2006) Densification and microstructural evolution of  $\text{TiO}_2$  films prepared by sol-gel processing. *Chem Mater* 18:4478–4485
- Löbmann P, Röhlen P (2003) Industrial processing of  $\text{TiO}_2$  thin films from soluble precursor powders. *J Glass Sci Technol* 76:1–7
- Löbmann P (2005) Soluble powders as precursors for  $\text{TiO}_2$  thin films. *J SolGel Sci Tec* 33:275–282
- Chrysicopoulou P, Davazoglou D, Trapalis C, Kordas G (1998) Optical properties of very thin (<100 nm) sol-gel  $\text{TiO}_2$  films. *Thin Solid Films* 323:188–193
- Matsubara T, Oishi T, Katagiri A (2002) Determination of porosity of  $\text{TiO}_2$  films from reflection spectra. *J Electrochem Soc* 149(2):C89–C93
- Mechiakh R, Bensaha R (2006) Variation of the structural and optical properties of sol-gel  $\text{TiO}_2$  thin films with different treatment temperatures. *C R Physique* 7:464–470
- Krüger R, Glaubitt W, Löbmann P (2002) Structural evolution in sol-gel-derived yttrium aluminum garnet-alumina precursor fibers. *J Am Ceram Soc* 85:2827–2833
- Bockmeyer M, Herbig B, Löbmann P (2009) Microstructure of sol-gel derived  $\text{TiO}_2$  thin films characterized by atmospheric ellipsometric porosimetry. *Thin Solid Films* 517:1596–1600